Efficient Magnetic-Thermal Coupled Simulation of Electrical Machines using a double combined FEM-circuit approach

J. Driesen, R. Belmans K. Hameyer
Katholieke Universiteit Leuven,
Dep. EE (ESAT), Div. ELEN
Kardinaal Mercierlaan 94
B-3001 Heverlee, BELGIUM

A. Arkkio, T. Jokinen
Helsinki University of Technology
Laboratory of Electromechanics
P. O. Box 3000
FIN-02015 HUT, FINLAND

Abstract

A computationally efficient simulation algorithm to simulate of the coupled magnetic-thermal field of electric machines is proposed. This algorithm uses a combined FEM-circuit approach in both, magnetic and thermal field regions.
A FEM (finite element method) calculation is used to compute phenomena in a 2D-cross-section, whereas the circuit approach is applied to consider phenomena in the axial z direction with an appropriate accuracy. The coupling between these four sets of equations results in a computationally efficient method. This is illustrated by means of the simulation of a 15 kW four-pole TEFC induction machine.

1 Introduction

In order to obtain accurate simulations in the design stage of electrical machines, an approach coupling simulations of different physical fields is recommended. Especially the coupling between the magnetic and the thermal field inside the machine is important. The ohmic, eddy current and iron losses are heating the machine, influencing the overall performance of the machine. E.g. induction machines are encountered with changes in the resistivity of the bars and windings, resulting in altered time constants affecting the control performance of a high-performance drives.
Coupled simulations are leading to improved models and approximations of the overall machine behaviour.

2 Magnetic field simulation

2.1 Magnetic field equation

The calculation of magnetic fields inside electrical machines has become common practice. Mainly the FEM-based methods, derived from a time-harmonic or a time-stepping formulation are used for this purpose. Eq. (1) shows the vector potential equation from which the vector potential is calculated.

$$\nabla\left(\upsilon(A,T)\nabla A\right) - j\omega\sigma(T)A + \frac{\sigma(T)}{\nu_0}\nabla(V) = 0 \qquad (1)$$

with:

A : z-component of the vector potential
V : electrical potential across the conductor
υ : reluctivity
σ : electrical conductivity

The magnetic material reluctivity has to be described non-linearly when saturation is considered. The thermal dependence of the electrical conductivity occurring in both magnetic and electrical circuit parameters lead to a non-linear coupling with the thermal field.

2.2 Machine modelling

Due to the construction of cylindrical rotating electrical machines, a 2D model allows an accurate simulation. Phenomena observed in the third dimension, such as the influence of the stator end-winding and the rotor end-ring of an induction machine, are taken into account by coupling the FEM-model with extra algebraic circuit equations [1]. This brings the extra unknowns V representing the electrical potential into eq. (1), leading to expressions for the current density.
A full 3D-model of the machine is seldom computed. Detail 3D-models are used to study end-effects from which the values of the circuit parameters can be deducted [2].

3 Thermal field simulation

3.1 Thermal field equation

The heat generated inside an electrical machine originates from different sources. The losses are determined based on the results of the magnetic calculation. Therefore, they lead to coupling terms (eq. (2)).

$$\nabla\left(k(T)\nabla T\right) = -\frac{J_s^{\,2}}{\sigma(T)} - p_{Fe} + \sigma(T)\omega^2 A^2 \qquad (2)$$

with k the thermal conductivity.

The source terms on the right-handside represent the joule losses by applied current, the iron loss, the eddy current loss and the external losses.

3.2 Comparison of thermal simulation methods

Thermal models for electrical machines have a long history [3]. The circuit approach (thermal networks) was prevailing. This method offers a fast and robust calculation of the temperatures inside electrical machines, especially when T-shaped networks are applied to model solid components [4].
However, together with FEM-based methods in magnetic calculations, thermal FEM-based calculations are increasingly applied [5]. The difficulties in these models are the correct representation of insulations, contact resistances and the heat transfer through the air gap.
These models can be considered two-dimensional in a plane perpendicular to the shaft or axisymmetric to approximate the heat flow through the casing, bearings and end-regions. Simplified 3D FEM-models exist as well [6], covering only part of the machine.

3.3 Fluid flow models

In general, the heat transport perpendicular to the shaft of the machine can be modelled with an acceptable accuracy in both methods. Heat transfer models describing the fluid flow in the air gap are applied to acquire an appropriate thermal resistance element or to derive equivalent material filling parameters for the air gap elements.
Models for the external cooling flow in between the cooling ribs lead to applicable convection coefficients.
Less is known about the effects influencing the heat flow in the axial direction. For example, the flow of the cooling fluids in the end-regions is very complex. Therefore, 3D-calculations should be coupled to a 'computational fluid dynamics'-simulation (CFD), requiring huge computational efforts. The circuit approach offers the advantage that the heat transport in the axial direction is modelled in a straightforward way, using thermal resistances. The determination of their values is troublesome and asks for experience and measurements.

3.4 Combination of the lumped parameter and FEM approaches

Combining the FEM-approach for radial 2D-models and circuit models for the axial dimension enables the use of the well-known methods to model radial heat flow and the possibility to take advantage of the experience about modelling the axial thermal phenomena (fig. 1).
This approach enables the construction of symmetric or asymmetric thermal models. Symmetric models do not consider differences in the cooling between the driving-end and the non-driving-end with the consequence that the machine does not contain temperature differences along the axis which can be an acceptable assumption for short machines. Asymmetric models can be built up by providing different circuits at the front and the rear side of the FEM model.
The anisotropy in the thermal conductivity due to the stacking of the cores is considered in this simple method.
If it were appropriate to divide the machine in several sectors, e.g. each with its own convection constraints, several FEM-slices, one for each sector, could be connected by a thermal circuit in the axial direction.

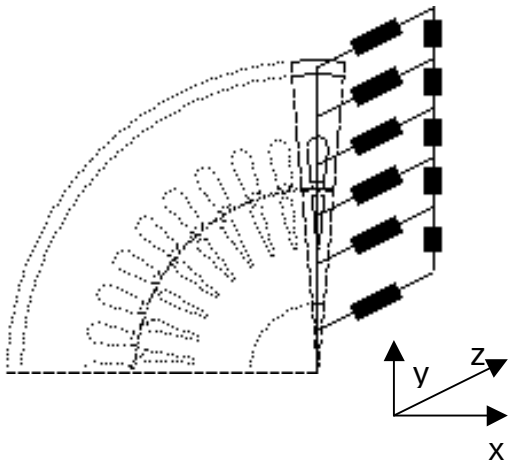

Fig. 1: Principle of the combined thermal FEM-circuit-model; Resistances shown in the model represent the axial thermal phenomena.

4 Coupling of the magnetic and thermal simulations

The calculations in the magnetic and the thermal domain result in four sets of non-linear equations to be coupled numerically:

- magnetic FEM-equations
- electrical circuit equations
- thermal FEM-equations
- thermal circuit equations

This coupling can be accomplished in different ways.

4.1 Cascade iteration

A first possibility is a cascade iteration algorithm in which the systems are solved one after another [5, 7].
This may result in a poor convergence of the non-linear iteration loop and advanced relaxation has to be applied. On the other hand complicated loss calculation algorithms can be introduced easily.

4.2 Fully coupled iteration

A second possibility is a fully coupled large system of equations in which the four sub-sets are placed, together with interface equations. Due to the different numerical properties of the sub-problems, this may result in a very ill-conditioned system of equations, requiring advanced equation solvers to obtain acceptable convergence. A larger amount of memory is required also.
To cope with the non-linearities, two non-linear iteration strategies can be followed:

- *Piccard iteration*: successive substitution requiring only function evaluation.
- *Newton-Raphson iteration*: the partial derivatives of the non-linearities have to be known for every field type, so a good knowledge of the material

characteristics and an appropriate linearisation of the heat source terms is necessary; the reward is a (usually) faster convergence.

4.3 Intermediate approaches

An intermediate approach is possible by placing the FEM-equations together with their corresponding circuit equations in one system describing a single physical domain. These 'physical' sub-systems are then coupled in a cascade-like iteration. Problem-own non-linearities such as saturation in the magnetic sub-problem, are treated locally, by a relatively fast iteration.
This method has a moderate rate of convergence, but requires less memory and is still very flexible.
From a computationally point of view this method is very efficient since most of the time the derivatives necessary to start up a Newton method can be obtained rather easily within one field (e.g. saturation characteristics in the magnetic sub-problem). The partial derivatives for the coupling terms are more difficult to obtain. Therefore, within the inter-field iteration loop, a relaxed substitution algorithm is used whereas within the individual physical fields Newton iteration is employed.

5 Electromagnetic-thermal coupled simulation of an induction machine

5.1 Induction machine

A magnetic-thermal coupled calculation of a four-pole TEFC (totally enclosed fan-cooled) induction machine is studied. The rotor is constructed with a number of slots which is not a multiple of the number of poles, thus half of the machine has to be modelled (fig. 2).
Relevant motor data can be found in table 1.

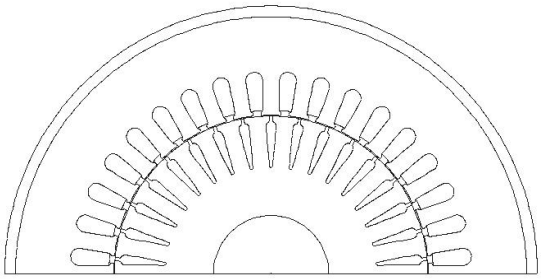

Fig. 2: Model of the 4-pole induction machine.

Table 1: Properties of the induction machine.

Power	15 kW
Rated speed	1450 rpm
Rated torque	98.8 Nm
# of stator slots	36
# of rotor slots	34
Rated voltage	660/380 V
Rated current	17.3/30 A (cos φ=0.86)

This model is meshed 21534 first order triangular elements (fig. 3). The same mesh is used for the thermal as well as the magnetic field. It is constructed by starting the calculation on a rough mesh and then applying h-adaptation based on relevant error estimators. In the following iteration steps this mesh is retained. The boundary conditions are of the Dirichlet type at the outer surface of the frame. On the two parts of the motor shape periodic boundary conditions are applied to support the symmetry.

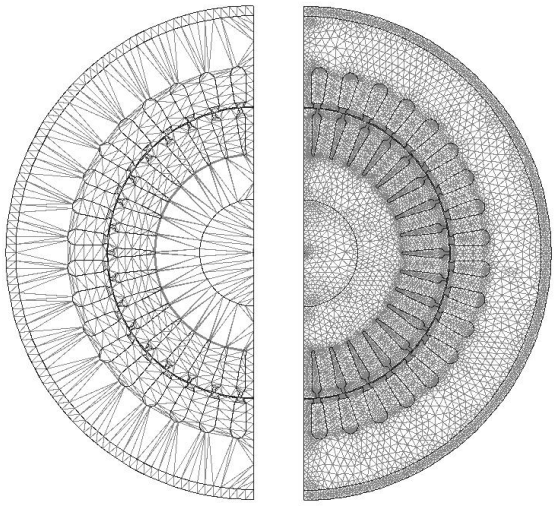

(a) Initial mesh (b) refined mesh

Fig. 3: Mesh used to model the 4-pole induction machine.

Different meshes may be used to save elements in a sub-problem, but in that case extra projection methods have to be applied.
To solve the coupled problem for a full load situation by a double combined FEM-circuit approach, the intermediate iteration strategy is used, along with adaptive relaxation to obtain convergence. The stop criterion is based on the $\|\bullet\|_\infty$-norm of two consecutive solution vectors at the end of the iteration loop.

5.2 Magnetic field

The time-harmonic magnetic model is coupled with voltage-driven circuit equations describing the effect of the end-windings, the bars outside the rotor and the end-rings requiring 96 lumped parameters. The circuit equations are put into one system together with the FEM-equations.
The natural difference of the circuit equations compared with the magnetic field equations causes a bad conditioned system of equations, but by using a robust equation solver, the solution is obtained after a relatively short computation time.

5.3 Thermal field: FEM part

Boundary conditions
The thermal model consists of an identical FEM geometry, except for different boundary conditions on the frame of the motor model. There, convection is applied, with a coefficient determined from literature [9] and corrected with measurements of the coolant flow. The convection coefficient is then multiplied with a cooling factor to account for the enlarged surface due to the ribs.

Conductor Modelling
The winding in the stator consists of copper wires with an individual insulation. The thermal conductivity of the equivalent winding material in the winding mesh elements is derived from eq. (3) [8].

$$k_{eq} = k_{in}\left(\frac{d_c}{d-d_c}+\frac{d-d_c}{d}\right) \qquad (3)$$

with k_{in} thermal conductivity of the insulation, d diameter of the insulated wire and d_c conductor part of the wire.
The rotor conductors are cast aluminium bars, thus no insulation has to be modelled.

Contact Resistance
The contact resistances can be modelled in three different ways.

1. Apply a correction to the thermal conductivities of the conductor materials. This causes an error in the internal temperature distribution of the conducting region, but the average temperature is correct. This temperature is then used to update material data of the related subproblems. Despite the extra averaging, this approach has the advantage that there is a clear geometrical relation between the elements of those regions in the different sub-problems, being advantageous for the projection methods.
2. Insert an extra equivalent contact layer of elements and fill these with an equivalent contact material. In order to obtain an acceptable aspect ratio of the finite elements, many elements have to be put in the contact layer and adjacent regions. Due to the high number of slots and the small size of the contact layer, this yields a significant growth of the model and hence the computation time. The number of elements can be reduced if the layer is enlarged, but this reduces the size of the conductor and the tooth, so no clear geometrical relationship exists anymore between the thermal and the magnetic sub-problem. If the same model, with the reduced conductor, would be used for the magnetic subproblem, an error would be made in the leakage flux and the joule heat calculation.
3. Duplicate the nodes lying on the edges marking the border between the conducting region and the iron. Extra algebraic equations modelling the contact are inserted to define the thermal relationship of the nodes. The standard meshing algorithms need to be adapted to generate the extra nodes. Moreover these extra equations change the numerical properties of the matrix system to be solved.

The first approach is used here to compute the coupled fields in this machine.

Air gap representation:
An important part of the thermal model is the representation of the air gap. In the finite element model, the air is defined by an equivalent conductivity, of which the value is calculated based on fluid-dynamics considerations.
In a first step, the flow regime in the air gap is determined. The calculation of the Taylor number of the flow shows that no vortices arise and that the transport is laminar [9]. Hence the main heat transport mechanism in the air gap is conductive, being the basic heat transport mechanism described by eq. (1).
From experiments described in literature [10], a Nusselt number can be estimated for this flow. This has to be augmented by 20% because of the non-smooth surfaces causing recirculating flows. The non-smoothness of the rotor here has the largest influence.
This leads to an estimate for the surface heat transfer coefficients for the rotor and stator surface. For these types of flows, the temperature dependency of the parameters can be neglected.
In the classical lumped parameter thermal models, a series connection of two thermal resistances is calculated based on these values. To derive an equivalent thermal conductivity $k_{eq,air}$, it is assumed to be equal to a thermal resistance of an cylindrical component with the dimensions of the air gap.

5.4 Thermal field: circuit part

This FEM model is extended by a circuit part, thus introducing thermal paths connecting shaft, yokes, slots and frame through thermal resistances (lumped parameter models).

- Internal end-region in air: the circulating air in the end-region is assumed to have an equally distributed temperature.
- End-windings and end-rings enlarging the internally ventilated surface.
- Bearings; to this node a source element representing the bearing losses is introduced.
- End-caps, providing extra heat paths and ventilation surfaces.

The lumped parameter models are in a T-shaped form, as described in [4]. Details about the values of elements can be found in [11, 12].

The thermal field plotted in fig. 4 is obtained at the end of the overall iteration. The isothermal lines in the shaft are caused by heat flowing through it, a path described by a thermal network circuit equation.

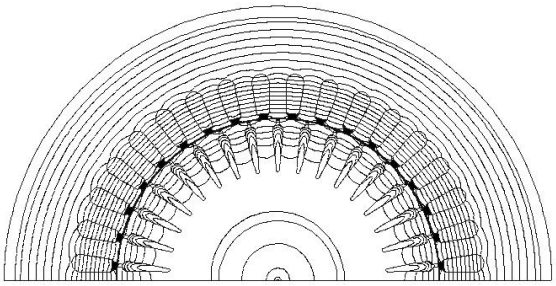

Fig. 4: Isothermal lines of the temperature distribution.

5.5 Results and discussion

Field plots obtained after convergence of the combined magnetic and thermal solution are found in fig. 4 & 5. The calculated torque amounts 94 Nm.
In the iteration loop the solution of the non-linear magnetic problem takes some minutes, whereas the linear thermal problem is solved in less than one minute.

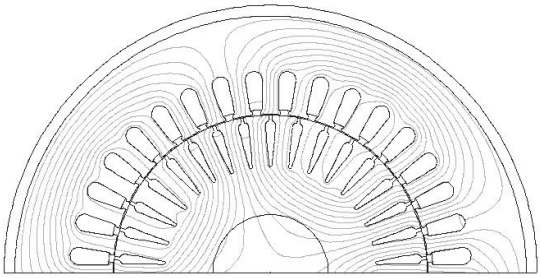

Fig. 5: Real part of the time-harmonic solution of the magnetic field (final solution after convergence of the iteration loop).

Table 2 contains temperatures extracted from the combined FEM-circuit model. The second column contains results obtained by solving a lumped parameter network model as described in [11, 12] and that has been experimentally verified. Since this model contains less than 100 unknowns, the solution time amounts only a few seconds being a lot less than the time necessary to solve an FEM-problem.

Table 2: Comparison of selected temperatures in the FEM model and the results of a thermal network. The minimum and maximum temperatures are given for the FEM-model.

Location	*FEM + circuit (°C)*	*Thermal network (°C)*	*Test (if available) (°C)*
Rotor bar	108	109	-
End-ring	132	132	141
Rotor tooth	105-107	108	-
Rotor yoke	106-107	108	-
Shaft	106	100	-
Stator winding	48-53	78	-
End-winding	80	80	93
Stator tooth	47-53	57	-
Stator yoke	43-47	42	-
Frame	42	35	45

In both models heat flows in the axial direction are found, for instance:

- heat transport through the shaft and the frame;
- the heat produced in the stator end-windings and rotor end-rings is partially convected to the air in the end-cap region, but a substantial part flows by means of conduction to the conductors in the core regions;
- the faces of the stator and rotor yoke are ventilated by the end-cap air.

A good agreement is found in table 2. The full lumped parameter thermal model requires less calculation time, due to the smaller solution vector, whereas the FEM-model is able to show more detail and hot spots. From the network model, only average temperatures are extracted, whereas the FEM model considers gradients influencing the local electromagnetic properties of the windings and therefore, leading to a more exact magnetic field solution as well.
However, it is more difficult to include effects like contact resistances in the FEM model, but specialised methods as described in the previous chapter can cope with that.

6 Conclusions

An efficient method to simulate coupled magnetic-thermal fields of electrical machines is presented. 2D FEM magnetic and thermal models are coupled to electric and thermal lumped parameter circuits to consider magnetic and thermal effects situated in the axial direction of the machine. With this approach an efficient and robust coupled field simulation scheme is presented.
This powerful method is demonstrated by means of a simulation of a four-pole TEFC induction machine which including the coupling of 2D discretised time-harmonic magnetic equations, electrical circuit equations modelling the windings, discretised thermal equations and equivalent thermal circuit models.

Acknowledgment

The authors are grateful to the Belgian “Fonds voor Wetenschappelijk Onderzoek - Vlaanderen” for its financial support of this work and the Belgian Ministry of Scientific Research for granting the IUAP No. P4/20 on Coupled Problems in Electromagnetic Systems. The research Council of the K.U.Leuven supports the basic numerical research. J. Driesen is a research assistant of the F.W.O.-V.

References

[1] A. Arkkio, "Analysis of the induction motors based on the numerical solution of the magnetic field and circuit equations," **Acta Polytechnica Scandinavica, Electrical Engineering Series No 59,** 1987, 97 p.

[2] R.De Weerdt, K.Hameyer, R.Belmans: "Parameter computation of squirrel-cage induction motor models using finite element," **10th Conference on the computation of electromagnetic fields (Compumag)**, Berlin, Germany, July 10-13.1995, pp.140-141.

[3] J. Hak, “Lösung eines Wärmequellen-Netzes mit Berücksichtigung der Kühlströme,” **Archiv für Elektrotechnik,** vol. 42, pp. 137-154, 1956.

[4] P. H. Mellor, D. Roberts, and D. R. Turner, “Lumped parameter thermal model for electrical machines of TEFC design,” **IEE Proceedings-B**, vol. 138, pp. 205-218, 1991.

[5] K. Hameyer, U. Pahner, R. Belmans, H. Hedia, “Thermal Computation of Electrical Machines,” **3rd international workshop on electric & Magnetic fields**, Liège, Belgium, May 6-9, 1996, pp.61-66.

[6] M. Plejic, B. Hribernik, “Parameter identification for FEM thermal models of electrical machines,” **Proc. ICEM ’96**, Vol. I, pp. 282-285.

[7] V. Hatziathanassiou, J. Xypteras, G. Archontoulakis, "Electical-thermal coupled calculation of an asynchronous machine," **Archiv für Elektrotechnik**, vol. 77, pp. 117-122, 1994.

[8] G. Gotter, "Erwärmung und Kühlung elektrischer Maschinen," **Springer Verlag**, Berlin, 1954.

[9] J. Saari, "Thermal Analysis of high-speed induction machines," **Acta Polytechnica Scandinavica, Electrical Engineering Series No 90,** 1998, 73 p.

[10] C. Gazley, "Heat-transfer characteristics of the rotational and axial flow between concentric cylinders," **Trans. of the ASME**, vol. 80, jan. 1958, pp. 79-90.

[11] M. Kaltenbacher, J. Saari, "An asymmetric thermal model for totally enclosed fan-cooled induction motors," **Laboratory of Electromechanics, Helsinki University of Technology, report no. 38**, Espoo, Finland 1992.

[12] T. Jokinen, J. Saari, "Modelling of the coolant flow with heat flow controlled temperature sources in thermal networks," **IEE-Proc. Electr. Power Appl.,** vol. 144, sept. 1997, pp. 338-342.